Exploring Transient Chaos in an NMR-Laser Experiment

Imre M. Jánosi,[1] Leci Flepp,[3] and Tamás Tél[2]
[1]*Department of Atomic Physics, Eötvös University, Budapest, Puskin u. 5-7, H-1088, Hungary*
[2]*Institute for Theoretical Physics, Eötvös University, Budapest, Puskin u. 5-7, H-1088, Hungary*
[3]*Physics Institute, University of Zürich, CH-8001 Zürich, Switzerland*
(Received 28 October 1993)

A time series analysis of transient chaos has been carried out in a laboratory experiment. The process is based on the construction of a long artificial time series obtained by gluing pieces of many transiently chaotic signals together. The strange saddle responsible for the transient chaotic behavior of an NMR laser has been reconstructed. Characteristics like dimension, Lyapunov exponent, and correlation function are determined showing that the motion on this set is more unstable than on the coexisting chaotic attractor.

PACS numbers: 05.45.+b, 06.50.Dc, 76.60.–k

Before the phenomenon of deterministic chaos was discovered, strongly fluctuating, erratic experimental signals were traditionally discarded as physically uninteresting noise. In the last two decades new methods have been developed which make it possible to exploit the structure hidden in chaotic time series in a systematic way [1]. The present state of affairs with *transient signals* is very much similar to that with permanent chaos in the past. Very often initial transients are still considered as switching on or warming up effects.

In this paper we demonstrate that the presence of transients is often a consequence of inherent dynamical properties of nonlinear systems, and their proper evaluation yields basic physical information. The appearance of chaos on finite time scales is known as *transient chaos* (for a review see [2]), and provides an example of a kind of "nonequilibrium process" that cannot be understood as an asymptotic behavior. In such cases one observes a moving around of the system in an apparently chaotic manner and then, rather suddenly, a settling down to a steady state which is either a periodic or a chaotic motion.

Transient chaos is closely connected to many other aspects of nonlinear dynamics. For scattering processes in open Hamiltonian systems chaos is inevitably of transient type and *chaotic scattering* [3] has attracted great recent interest. *Diffusion* and other transport phenomena can also be interpreted as consequences of chaotic scattering [4]. In dissipative cases, the so-called *noise induced chaos* [5], when a system with simple attractors turns chaotic in the presence of noise, has recently been explained as a consequence of transient chaos [6]. Transient chaos can also be a sign of permanent chaos to be born. More generally, all types of crisis configurations, attractor destructions, explosions, or mergings [7], are accompanied by long lived chaotic transients.

In physical systems exhibiting transient chaos there exists in phase space a *nonattracting chaotic set, a chaotic saddle* [2,7], that in dissipative cases coexists with an attractor. Trajectories starting from randomly chosen initial points then approach the attractor with probability 1. Because of the saddle's stable foliation, however, they might come close to the saddle and stay in its vicinity for a shorter or longer time, before reaching the attractor. This results in the appearance of a chaotic motion with a well defined average lifetime of $1/\kappa$ where κ is the escape rate, a basic characteristic of the chaotic saddle.

The experimental investigation of transient chaos has received, in spite of its relevance, relatively little attention (for a few examples, see [8,9]) and, with the exception of a very recent effort [9], has mainly concentrated on determining the average chaotic lifetime. In this paper we illustrate that transient chaos can be analyzed from time series in very much the same manner as permanent chaos. Chaotic saddles underlying transient chaotic dynamics can be reconstructed and their characteristics taken with respect to the natural measure can be determined from time series. To our knowledge, this is the first realization of such an analysis in a laboratory experiment where the underlying equations of motion are not used explicitly.

We have applied a method proposed in Ref. [10] for reconstructing chaotic saddles from experimental time series of one single variable. It is based on the creation of a long signal with transient properties and can be summarized as follows:

(a) Take an ensemble of time series containing transients to a steady state behavior.

(b) Locate the attractor of the dynamics in the variable investigated and separate the transient parts.

(c) Construct truncated time series, i.e., drop those points of the transient that belong to the transition either from the initial point to the saddle or from the vicinity of the saddle to the attractor. The truncated time series generate a natural measure [11], and their average length is the reciprocal value of the escape rate from the chaotic saddle. The results obtained by an appropriate truncation should be insensitive to any additional truncations.

(d) By means of some simple matching procedure, glue the truncated signals together, apply a low-dimensional time-delay coordinate embedding, produce a Poincaré section, and plot the invariant set. The gluing process is

0031-9007/94/73(4)/529(4)$06.00

inevitably an excess noise source whose effect can, however, be kept under control (see Ref. [10]).

(e) Apply the usual time series analysis method to determine quantitative characteristics of the chaotic saddle.

The signals we investigated have been obtained from an NMR laser whose chaotic behavior has been studied for over a decade [12]. The low noise and drift free data made the system appropriate for an experimental investigation of a variety of phenomena, such as periodic orbits [13], templates [14], a heteroclinic crisis [15], noise reduction [16], or the control of chaos [17]. The detailed description of the experimental setup is available in the literature (see, e.g., [16]); here we just mention the features most relevant for our subject. Chaotic motion can occur in the NMR laser when the cavity quality factor $Q(t)$ is sinusoidally modulated, i.e., $Q(t) = Q_0[1+p\cos(2\pi\nu_m t)]$, where p (the control parameter) is the modulation amplitude, $\nu_m = 100$ Hz is the modulation frequency, and $Q_0 = 300$ is the quality factor of the free running NMR laser. The laser output is a time-dependent voltage.

Our investigations were carried out at a control parameter value just below the crisis point [15] and at a pump magnetization $M_e = -0.74$ A/m. It must be stressed that we chose the system parameters Q_0 and M_e different from $Q_0 = 330$ and $M_e = -0.78$ A/m used in previous publications [13,17]. The heteroclinic crisis at $p = p_c$ results in an attractor explosion. At $p < p_c$, close enough to the crisis point, the original (small) attractor coexists with a chaotic saddle; consequently, the steady state motion on the attractor occurs after a chaotic transient. Above the crisis point an enlarged strange attractor appears which incorporates both the former chaotic saddle and the attractor. The data for our analysis have been taken in the range $p < p_c$.

The laser transients were generated by changing the quality factor Q_0 in the following way: After reaching the chaotic steady state with some value $Q_0 = Q_i$, the quality factor was lowered to a given value Q_q resulting in a quenched state and kept at this value for a time of approximately $t_q = 5$ ms. Then, the quality factor was switched back to its original value Q_i and the laser output was recorded as a normalized, dimensionless scalar time series $\{\xi_1, \xi_2, \ldots, \xi_n\}$, $0 < \xi_i < 1$ of length $n = 1024$. The sampling frequency was 2500 Hz. The time series analysis was then carried out by following the steps of the scenario described above.

Step (a): An ensemble of 9599 short records has been generated. The length of these records ($t = 0.4096$ s) was chosen to be about 4 times the average chaotic lifetime, so that we have just a few signals exhibiting transient chaos during the full record. Another, smaller ensemble of only several hundred longer ($t = 1.9968$ s) transient records was used to prove that the probability to find transients on longer time scales was negligible. To characterize the chaotic steady state, a long series of 256 000 data was also recorded.

Figure 1(a) shows a typical segment of the steady

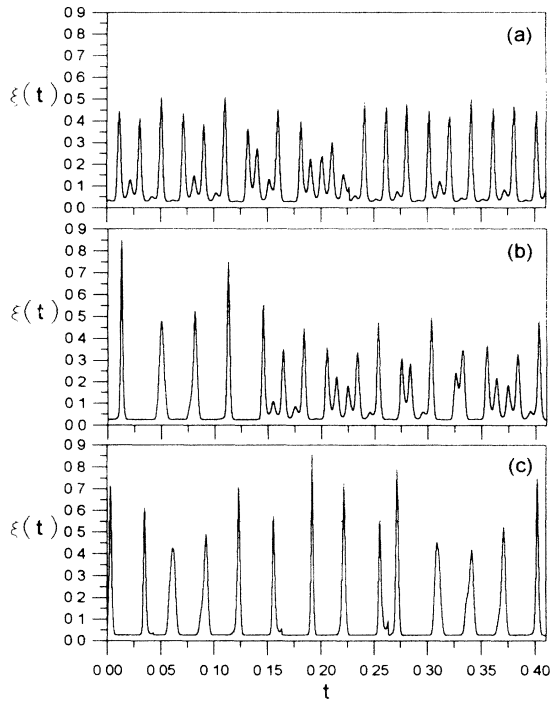

FIG. 1. Typical time series segments $\xi(t) \equiv \xi_i$ with $t = i(4 \times 10)^{-4}$ s consisting of 1024 data points (a) representing the steady chaotic motion on the attractor, (b) illustrating a typical transient, and (c) showing a piece of the artificial long time series representing the motion near the chaotic saddle. The dotted line represents the maximum measured value of the laser signal in the chaotic steady state.

chaotic signal. The dotted line denotes the maximum observed peak height in this state. Figure 1(b) illustrates a typical transient behavior. Switching back the quality factor at $t = 0$, a few peaks of relatively large amplitude arise after a delay time of approximately 0.02 s. The laser action between subsequent pulses is almost quenched. The various transient pieces will be glued together at this very low laser amplitude, the laser background level. The apparently chaotic motion outside the attractor then settles down to the steady state. Note that between the large transient impulses there are no peaks of intermediate amplitude characterizing the motion on the inner loop of the attractor [see Fig. 3(a) below].

Step (b): To separate the transient parts, we have applied the following empirical rule: Find the last peak of amplitude larger than the maximal observed amplitude at the steady state [dotted line in Fig. 1(b)] and keep the segment ending with this peak and a short piece of the laser background after. (The average distance between the peaks of the transient is ≈ 0.04 s with a random distribution; thus, the length of the short pieces added to the last peak was chosen to be 0.02 s.) Some information has been lost in this way because the last transient impulse may be smaller than the cutting level.

Step (c): The empirical rule we used also ensured discarding the transients from the vicinity of the saddle to

the attractor. In order to obtain truncated time series, the transients toward the saddle are also to be discarded. Because of the rather large modulus of the first negative Lyapunov exponent governing this decay (see below), it was sufficient to drop a little piece before the first large peak only. A careful investigation of the truncated time series shows that the probability to find a piece of length T decreases exponentially with T. The number $D(T)$ of truncated signals of lengths T is plotted in Fig. 2, after applying a local averaging. An exponential fit gives the escape rate $\kappa = 9.27 \pm 0.06\ \mathrm{s}^{-1}$.

Step (d): To decrease the noise coming from the gluing procedure, short truncated signals were discarded. Those longer than three effective periods of evolution (≈ 0.12 s), which is on the order of $1/\kappa$, have been glued together at the background signal level between the peaks. Figure 1(c) shows a segment of the long artificial time series of 2 037 577 data points obtained from 5608 truncated signals in this way. The differences between the steady state [Fig. 1(a)] and this motion are clear.

Step (e): A time series analysis of this artificial signal has been carried out. First we show in Fig. 3(a) the return map of the time series representing the motion near the chaotic saddle. A single peak (between the rising and falling edges) consists of typically 20–30 data points; thus the correlation is very high between consecutive data points. Therefore $\Delta n = 5$ was chosen in a two-dimensional time-delay embedding. This is to compare with Fig. 3(b), in which the return map of the coexisting chaotic attractor is plotted. Figures 3(c) and 3(d) display the Poincaré section of the saddle and the attractor, respectively, in a three-dimensional embedding. Careful inspection shows that the inner structures of the Poincaré sections are not identical at all; however, the branches of the saddle are close to the attractor. The presence of a low dimensional invariant set is clear in all cases. Note that the chaotic saddle has a larger extent than the attractor.

The effect of the gluing procedure on the Poincaré map [Fig. 3(c)] can be estimated by noticing that gluing takes place at the laser-background level. The artificial gluing points thus lie in a narrow region close to the origin of the pseudo phase space, and do not appear on the Poincaré plane. As a consequence, there might be a slight shift of the Poincaré points because of the fluctuations of the laser-background level but this induces a relative error of less than 1% only. The reliability of the computation of other characteristics based on the artificial time series (see below) is also due to this fact.

For the reconstruction of the static picture of the saddle, as appropriate for a dimension analysis, it is not necessary to glue together the truncated transient pieces forming a long time series. The advantage of this process appears definitely when one tries to characterize the chaotic saddle, since the standard algorithms developed for analyzing permanent chaos are applicable without any problem. As an example, we have used the Grassberger-Proccacia method [18] to obtain the correlation dimension. The embedding process, carried out up to ten dimensions, gives for the saddle $D_{\mathrm{corr}} = 2.30 \pm 0.1$ which coincides with the attractor dimension within error bars. The results also support the view that the system can be faithfully described in a three-dimensional phase space. As an independent check, we also determined the box dimension of the chaotic saddle appearing on the Poincaré plane obtained *without* gluing the truncated signals together. The result was indistinguishable from D_{corr} within error bars.

We also computed the Lyapunov exponents applying the Jacobian method [19] embedding the time series into

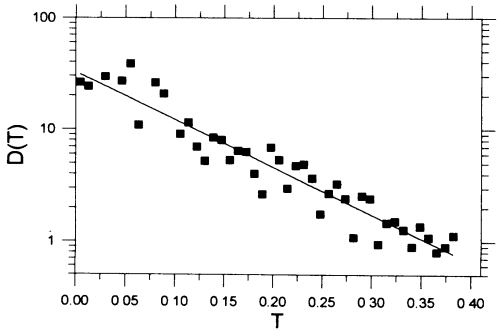

FIG. 2. Coarse grained lifetime distribution of the transients. The solid line shows the exponential fit: $D(T) = 34.23 \exp[-T/(0.1078\ \mathrm{s})]$. Time is measured in seconds.

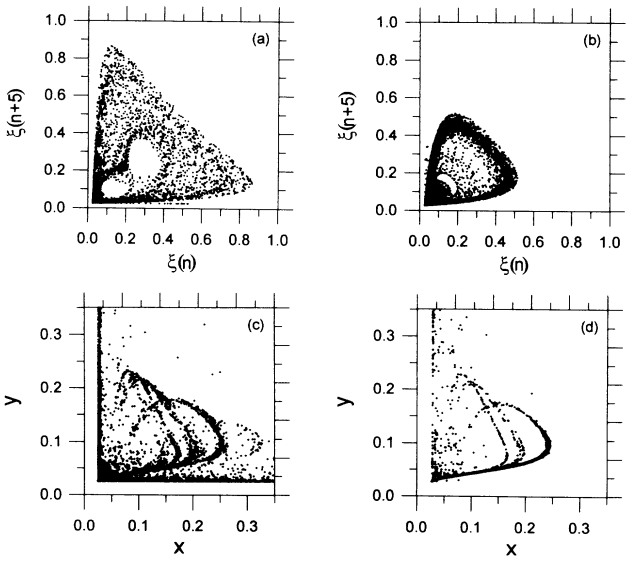

FIG. 3. Reconstruction of the invariant sets by the time delay embedding method. Return map for the saddle (a) and for the attractor (b). Poincaré section taken with the $z = 0.25$ plane in a three-dimensional time-delay embedding $\{x_i, y_i, z_i\} = \{\xi_i, \xi_{i+20}, \xi_{i+40}\}$ for the saddle (c) and for the attractor (d).

three dimensions. For the *maximum* Lyapunov exponent we obtained 225 ± 15 and $126.5 \pm 1.7\ s^{-1}$ for the saddle and the attractor, respectively. The higher value on the saddle shows that the divergence of nearby trajectories is much faster than on the attractor. The modulus of the negative Lyapunov exponent for both the saddle and the attractor is of order of $300\ s^{-1}$.

There is a famous formula [11] expressing the information dimension $D_1^{(u)}$ along the unstable manifold in terms of the escape rate κ and the maximal Lyapunov exponent λ_1 of the saddle in three-dimensional flows as $D_1^{(u)} = 1 - \kappa/\lambda_1$ which is expected to be close to the partial fractal dimension. With the values determined above, we obtain $D_1^{(u)} = 0.958 \pm 0.003$. Since this number is close to 1, the structure of the invariant set is not "airy"; i.e., it does not contain large holes.

As another illustration of the advantage of using long artificial time series, we plotted in Fig. 4 the autocorrelation function given by $A(t) = \langle \xi(t')\xi(t'+t) \rangle$. The most striking feature is that the motion on the chaotic attractor is more coherent than on the saddle. This is due to the presence of a densely populated inner and outer loop [see Fig. 3(b)] which is much less pronounced in the case of the saddle [Fig. 3(a)]. Consequently, a quasiperiodic behavior superimposed on the chaotic motion is observed, along with a much slower correlation decay than in the case of transient chaos. The situation is very much similar to the one found in a periodic window of the Hénon map where a 7-piece chaotic attractor coexists with a single chaotic saddle [10].

With these studies we hope to contribute to the establishment of transient chaos as an experimentally accessible phenomenon. It is very likely that many experimentally observed transient chaotic signals were considered in the past to be uninterpretable and were therefore discarded. This might be due to the fact that the asymptotic feature of chaos has been overemphasized, and the use of long time averages has been more common in the definition of chaos than that of ensemble averages. Moreover, the results obtained for the Lyapunov exponents or for the correlation decay strongly indicate that the motion on a chaotic saddle is *more chaotic* than the one on the coexisting strange attractor.

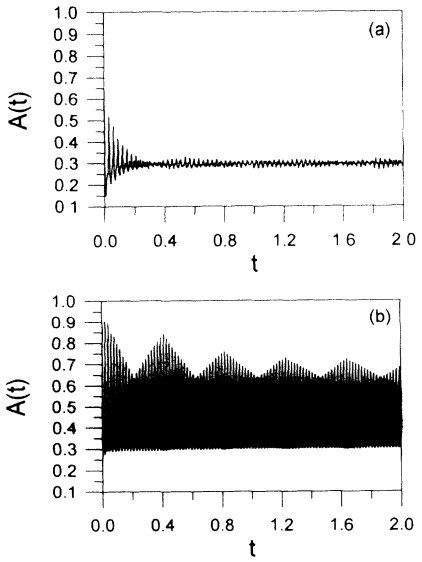

FIG. 4. Autocorrelation function $A(t)$ for the saddle (a) and for the attractor (b). Time is measured in seconds.

This work has been supported by the Hungarian National Science Foundation (OTKA) under Grant No. 2090, T4439. We also acknowledge very constructive collaboration with E. Brun, J. Simonet, and R. Badii, and partial support by the Swiss National Science Foundation and the Danish Science Academy.

[1] H. D. I. Abarbanel, R. Brown, J. J. Sidorovich, and L. Sh. Tsimring, Rev. Mod. Phys. **65**, 1331 (1993).
[2] T. Tél, in *Directions in Chaos*, edited by Hao Bai Lin (World Scientific, Singapore, 1990), Vol. 3, p. 149.
[3] U. Smilansky, in *Chaos and Quantum Physics*, edited by M. J. Giannoni *et al.* (North-Holland, Amsterdam, 1992), p. 121; "Chaotic scattering," Chaos **3**, No. 4 (1993).
[4] P. Gaspard and G. Nicolis, Phys. Rev. Lett. **65**, 1693 (1990).
[5] F. T. Arecchi, R. Badii, and A. Politi, Phys. Lett. **103A**, 3 (1984); M. Iansiti *et al.*, Phys. Rev. Lett. **55**, 746 (1985).
[6] A. Hamm, T. Tél, and R. Graham, Phys. Lett. A **185**, 313 (1994).
[7] C. Grebogi, E. Ott, and J. Yorke, Phys. Rev. Lett. **48**, 1507 (1982).
[8] P. Bergé and M. Dubois, Phys. Lett. **93A**, 365 (1983); F. T. Arecchi and F. Lisi, Phys. Rev. Lett. **50**, 1330 (1983); R. W. Rollins and E. R. Hunt, Phys. Rev. A **29**, 3327 (1984); R. C. Hilborn, Phys. Rev. A **31**, 378 (1985); R. W. Leven, B. Pompe, C. Wilke, and B. P. Koch, Physica (Amsterdam) **16D**, 371 (1985); D. Dangoisse, P. Glorieux, and D. Hennequin, Phys. Rev. Lett. **57**, 2657 (1986); T. L. Carroll, L. M. Pecora, and F. J. Rachford, Phys. Rev. Lett. **59**, 2891 (1987); Z. J. Kowalik, M. Franaszek, and P. Pieranski, Phys. Rev. A **37**, 4016 (1988); W. L. Ditto *et al.*, Phys. Rev. Lett. **63**, 923 (1989); P. J. Widmann, M. Gorman, and K. A. Robbins, Physica (Amsterdam) **36D**, 157 (1989); R. Stoop and J. Parisi, Phys. Rev. A **43**, 1802 (1991).
[9] R. W. Leven, M. Selent, and D. Uhrlandt (private communication).
[10] I. M. Jánosi and T. Tél, Phys. Rev. E **49**, 2756 (1994).
[11] H. Kantz and P. Grassberger, Physica (Amsterdam) **17D**, 75 (1985).
[12] E. Brun *et al.*, J. Opt. Soc. Am. B **2**, 156 (1985).
[13] L. Flepp *et al.*, Phys. Rev. Lett. **67**, 2244 (1991).
[14] N. B. Tufillaro *et al.*, Phys. Rev. A **44**, R4786 (1991).
[15] M. Finardi *et al.*, Phys. Rev. Lett. **68**, 2989 (1992).
[16] H. Kantz *et al.* Phys. Rev. E **48**, 1529 (1993).
[17] C. Reyl *et al.*, Phys. Rev. E **47**, 267 (1993).
[18] P. Grassberger and I. Proccacia, Physica (Amsterdam) **9D**, 189 (1983).
[19] Th.-M. Kruel, M. Eiswirth, and F. W. Schneider, Physica (Amsterdam) **63D**, 117 (1993).

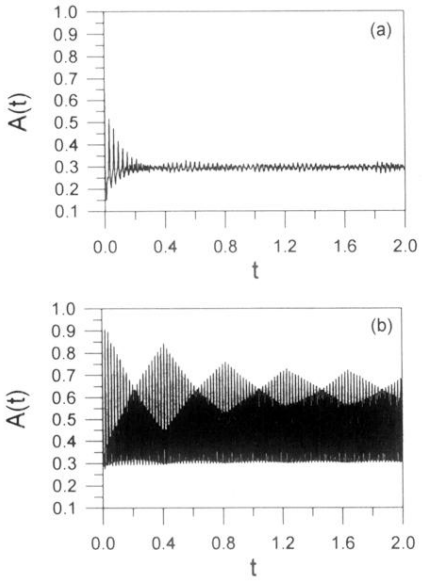

FIG. 4. Autocorrelation function $A(t)$ for the saddle (a) and for the attractor (b). Time is measured in seconds.